Supplementary: A Multi-Model Assessment of Evolving Forced Changes in Northern Hemisphere Modes of Atmospheric Circulation Variability and the Role of the Tropical Pacific

Nicola Maher, [1,2*], Clara Deser[3] and John P. O'Brien[4]

[1]Research School of Earth Sciences, Australian National University, Canberra, ACT, Australia.
[2]ARC Centre of Excellence for Weather of the 21st Century, Australian National University, Canberra, ACT, Australia.
[3]Climate and Global Dynamics Laboratory, National Center for Atmospheric Research, Boulder, Colorado, USA.
[4]Heising-Simons Foundation, Los Altos, California, USA.

*Corresponding author(s). E-mail(s): nicola.maher@anu.edu.au;

1 Model evaluation: Tropical Pacific

We evaluate the performance of the SMILEs in capturing the first two EOFs of tropical Pacific SST variability (Figure S1 & Figure 4 main paper bottom row). The first EOF exhibits a consistent pattern across all models and observations (correlations between 0.64 and 0.89 with observations); however, similar to the North Atlantic, the spatial maximum shifts between models. In contrast, the second EOF shows less agreement with observations (correlations between 0.3 and 0.78). While the broad-scale pattern is generally well captured, both the magnitude and finer details of the regression vary across models, indicating that this second mode is less well represented in the SMILEs compared to the first.

When examining the Tropical Pacific SST EOFs, our results align with previous studies (Figure S1 & Figure 4 mian paper bottom row). Most models show a high pattern correlation with observations for EOF1 (greater than 0.9), although the standard deviation is overestimated in some models (e.g. Planton et al, 2021; Bellenger et al, 2014). For example, in CESM1, CESM2 and MIROC6 all ensemble members

overestimate the standard deviation. For EOF2, model agreement with observations is generally weaker than for EOF1. However, all models except ACCESS-ESM1.5 have at least one member with a correlation around 0.8.

2 Supplementary Figures

References

Bellenger H, Guilyardi E, Leloup J, et al (2014) Enso representation in climate models: from cmip3 to cmip5. Climate Dynamics 42(7):1999–2018. https://doi.org/10.1007/s00382-013-1783-z, URL https://doi.org/10.1007/s00382-013-1783-z

Huang B, Thorne PW, Banzon VF, et al (2017) Extended reconstructed sea surface temperature, version 5 (ersstv5): Upgrades, validations, and intercomparisons. Journal of Climate 30(20):8179 – 8205. https://doi.org/10.1175/JCLI-D-16-0836.1, URL https://journals.ametsoc.org/view/journals/clim/30/20/jcli-d-16-0836.1.xml

Planton YY, Guilyardi E, Wittenberg AT, et al (2021) Evaluating Climate Models with the CLIVAR 2020 ENSO Metrics Package. Bulletin of the American Meteorological Society 102(2):E193 – E217. https://doi.org/10.1175/BAMS-D-19-0337.1, URL https://journals.ametsoc.org/view/journals/bams/102/2/BAMS-D-19-0337.1.xml

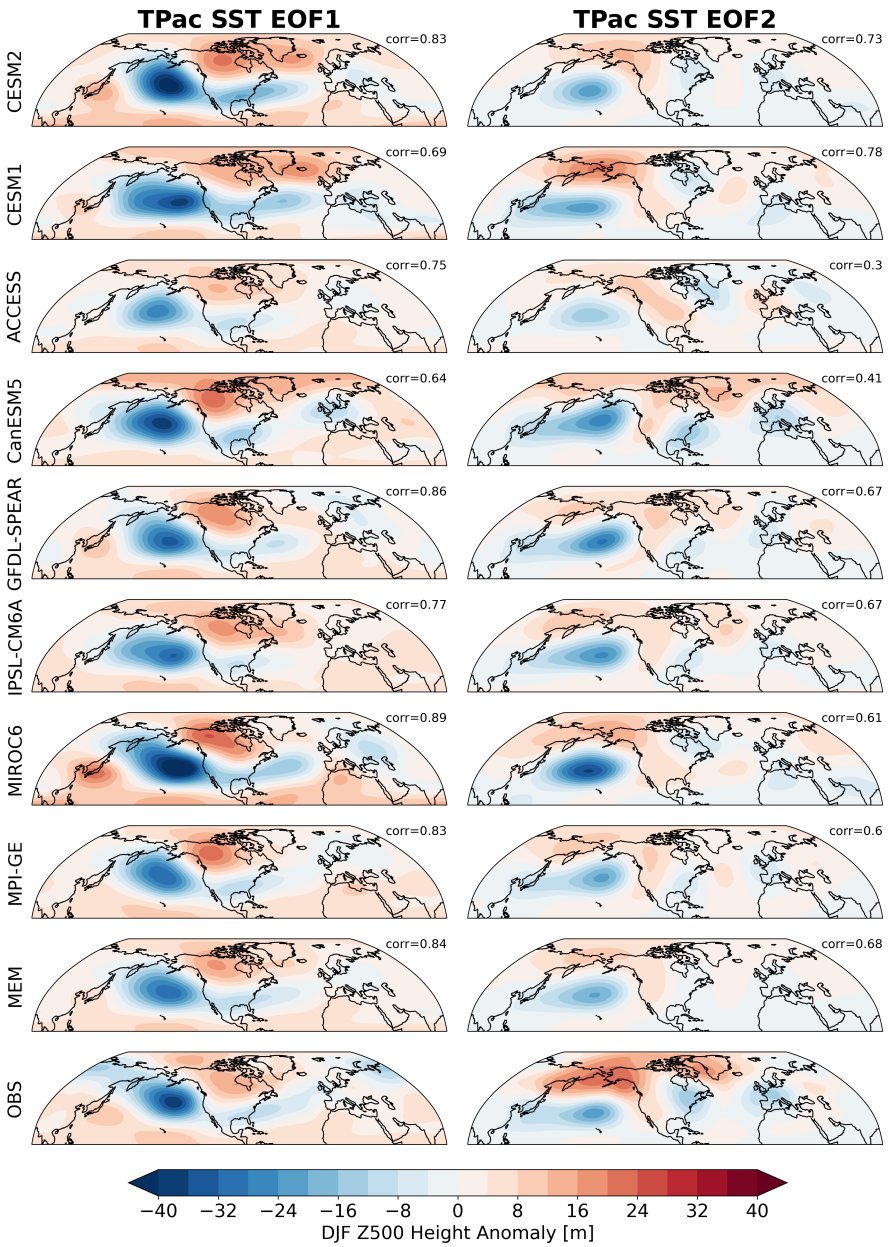


Fig. S1 EOFs for the Tropical Pacific SST regressed onto DJF Z500 anomalies for the observed period (1950-2015). Shown for 8 SMILES, the multi-ensemble mean (MEM, computed as the average of the eight SMILE regression maps) and observations from NOAA/CIRES/DOE 20th Century Reanalysis (V3). All computations are complete using a traditional time-based EOF approach, although results are qualitatively similar when SEOF's are used for the SMILEs (Figure S2). Observations are detrended by removing a quadratically fitted polynomial from each grid point, while the SMILEs are detrended by removing the ensemble mean. The pattern correlation of each map with the observed map is shown in the top right corner of each subplot.

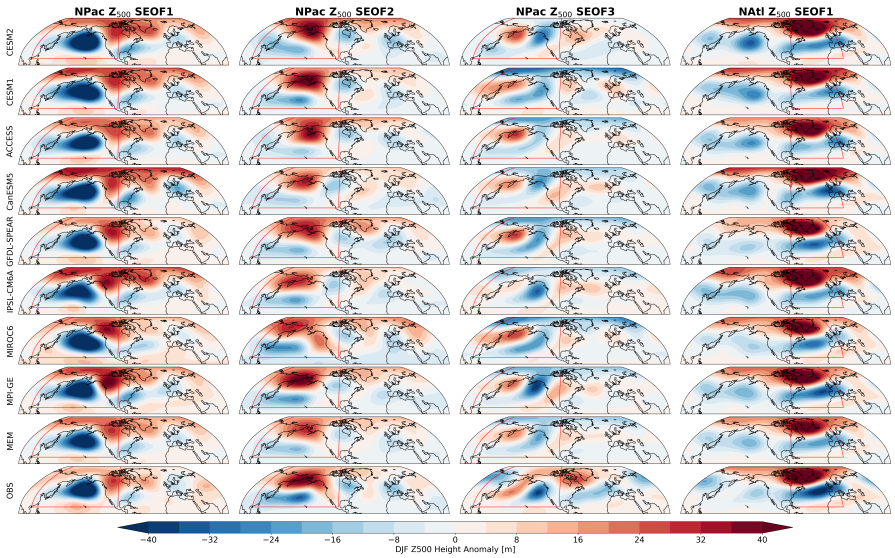


Fig. S2 SEOFs for the North Pacific and Atlantic Z500 regressed onto DJF Z500 anomalies for the observed period (1950-2015). Shown for 8 SMILES, the multi-ensemble mean (MEM, computed as the average of the eight SMILE regression maps) and observations from NOAA/CIRES/-DOE 20th Century Reanalysis (V3) and ERSSTv5 (Huang et al, 2017). Observations are detrended by removing a quadratically fitted polynomial from each grid point, while the SMILEs are detrended by removing the ensemble mean. The pattern correlation of each map with the observed map is shown in the top right corner of each subplot.

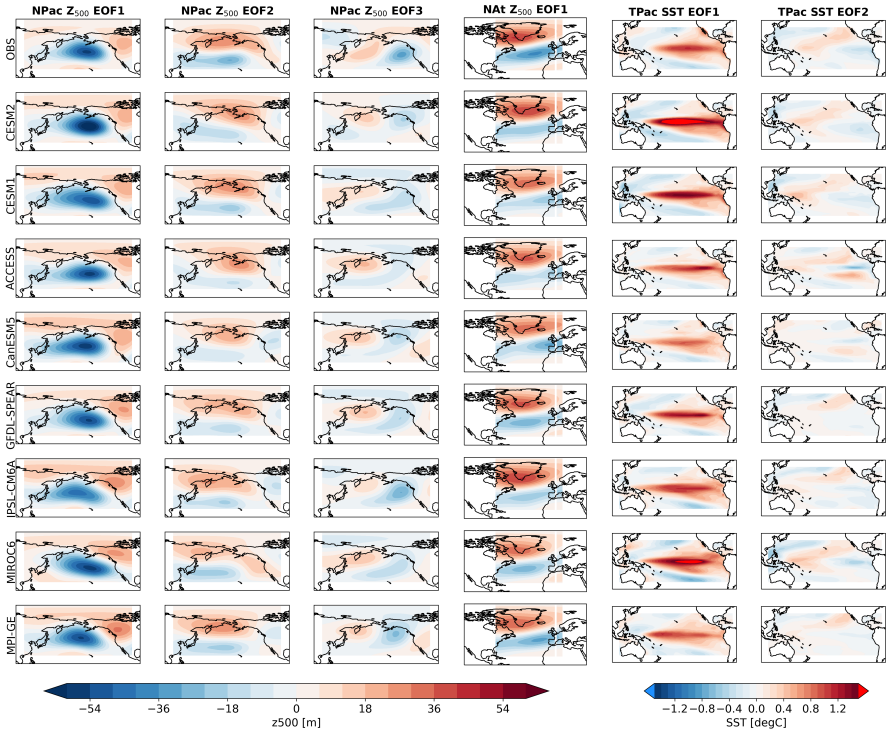


Fig. S3 EOF pattern for each SMILE and observations. Shown for North Pacific Z500 EOFs 1-3, North Atlantic Z500 EOF1 and Tropical Pacific SST EOFs 1-2. Z500 observations are from NOAA/CIRES/DOE 20th Century Reanalysis (V3) (1950-2015) and SST observations are from ERSSTv5 (1950-2015) (Huang et al, 2017). For this plot the EOFs are computed against time for the same period as the observations for each ensemble member. For this analysis the forced response is removed from the SMILE by removing the ensemble mean at each timestep. The observations are detrended using a quadratic fit. We note that detrending the SMILEs by removing a quadratic fit gives a qualitatively similar answer (not shown).

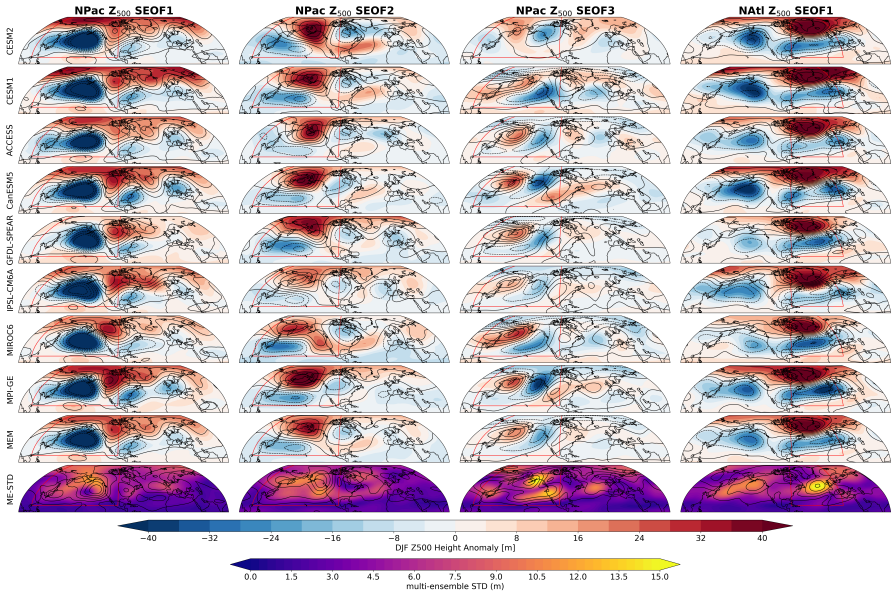


Fig. S4 Projection (full values rather than the change) in the North Pacific and North Atlantic Z500 SEOFs regressed back onto Z500. The North Pacific SEOF1-3 and North Atlantic SEOF1 as regressed onto Z500 from 2087-2097 compared to 1924-1934. Shown for each SMILE, the multi-ensemble mean (MEM) and the standard deviation across the 8 SMILE means. Contours show the baseline period 1924-1934 for reference.

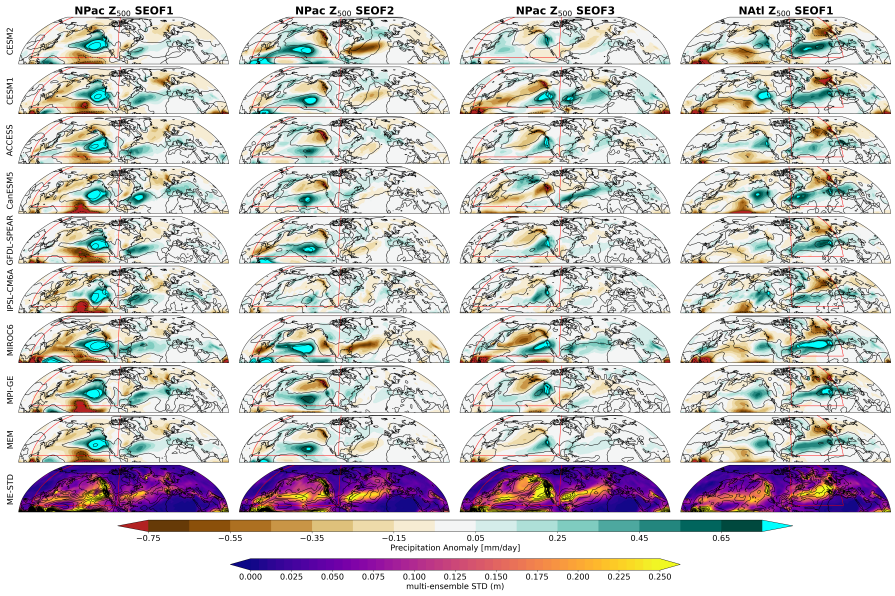


Fig. S5 Projection (full values rather than the change) in the North Pacific and North Atlantic Z500 SEOFs regressed back onto precipitation. As in Figure S4 but for precipitation.

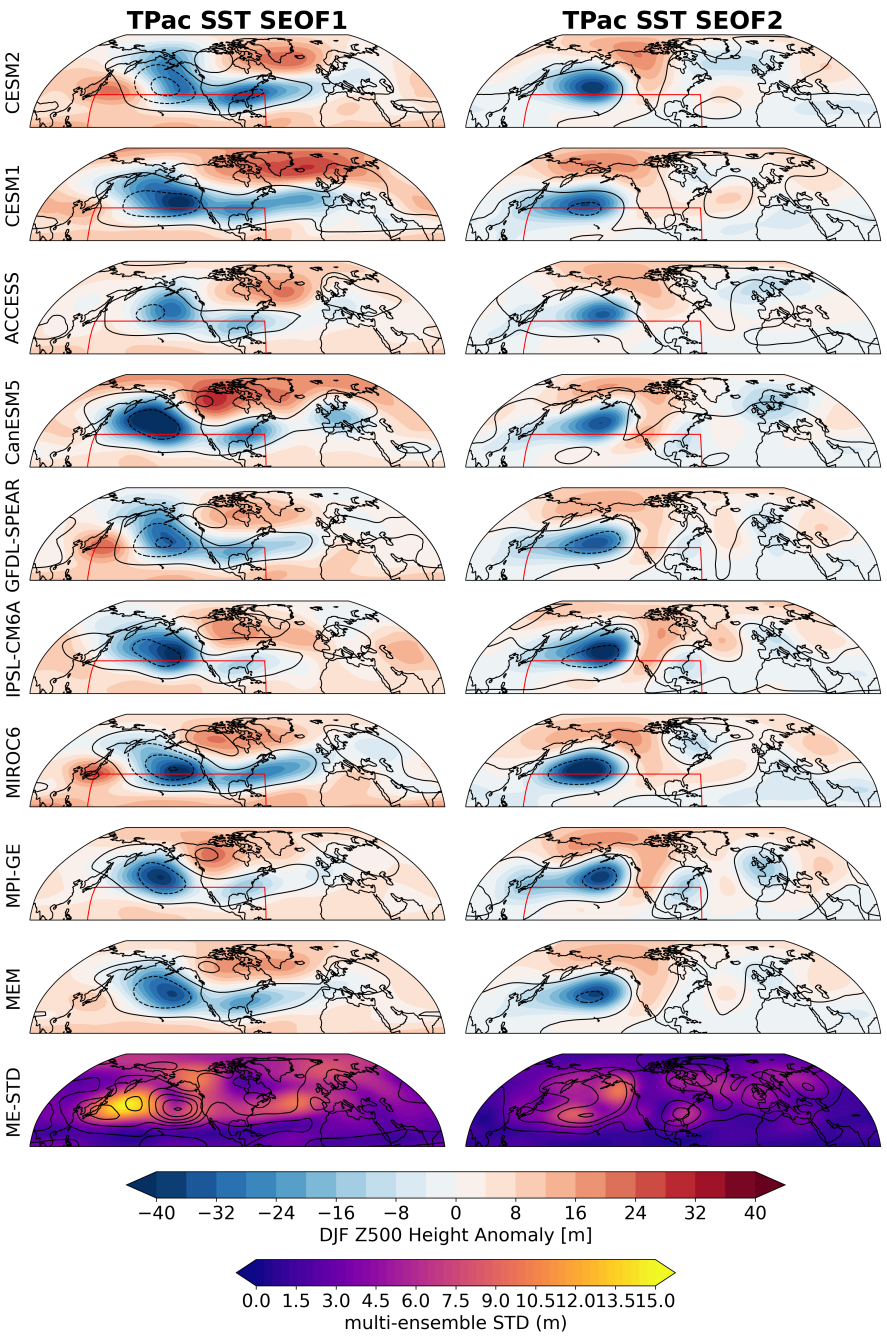


Fig. S6 Projection (full values rather than the change) in the Tropical Pacific SST SEOFs regressed onto Z500. The Tropical Pacific SEOF1-2 as regressed onto Z500 from 2087-2097 compared to 1924-1934. Shown for each SMILE, the multi-ensemble mean (MEM) and the standard deviation across the 8 SMILE means. Contours show the baseline period 1924-1934 for reference.

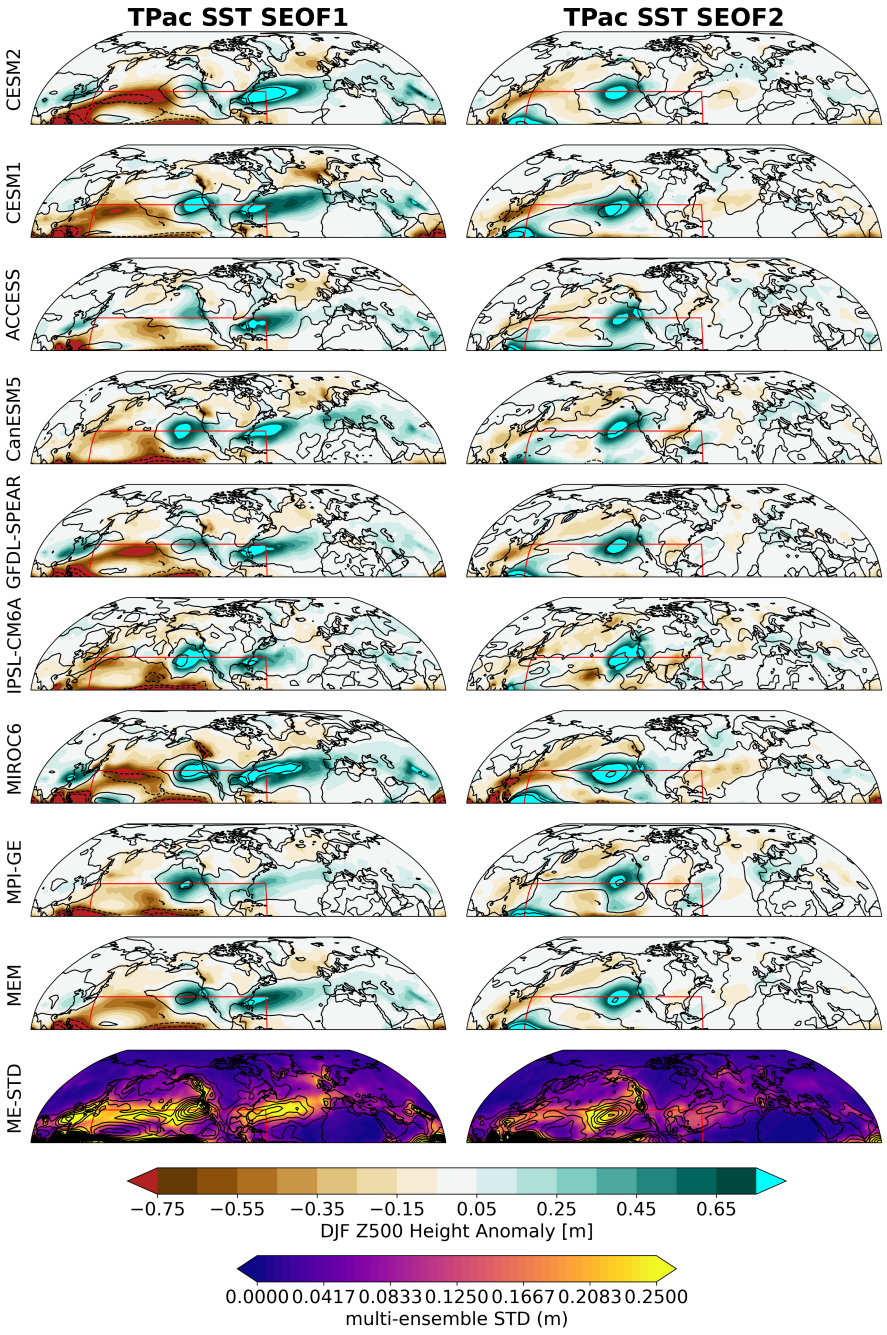


Fig. S7 Projection (full values rather than the change) in the Tropical Pacific SST SEOFs regressed onto precipitation. As in Figure S7 ranter but for precipitation.

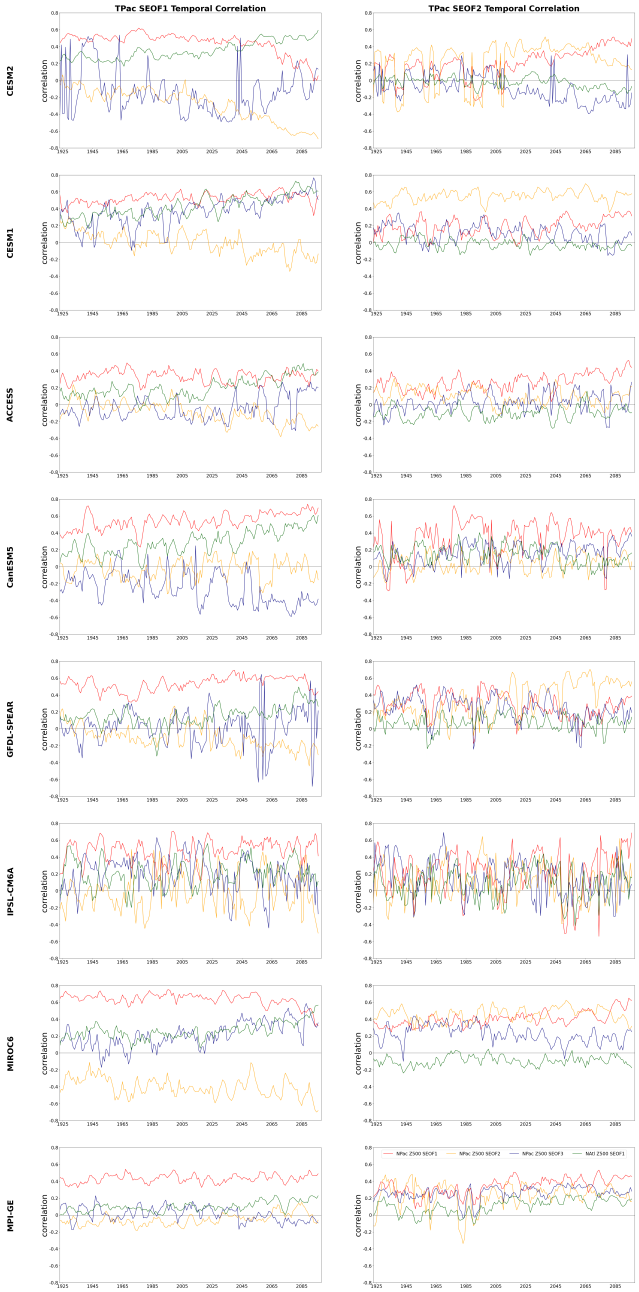


Fig. S8 Time-varying correlation coefficients between the SPC of each Northern Hemishpere Z500 SEOF mode and the SPC of Tropical Pacific SEOF1 (left) and 2 (right).

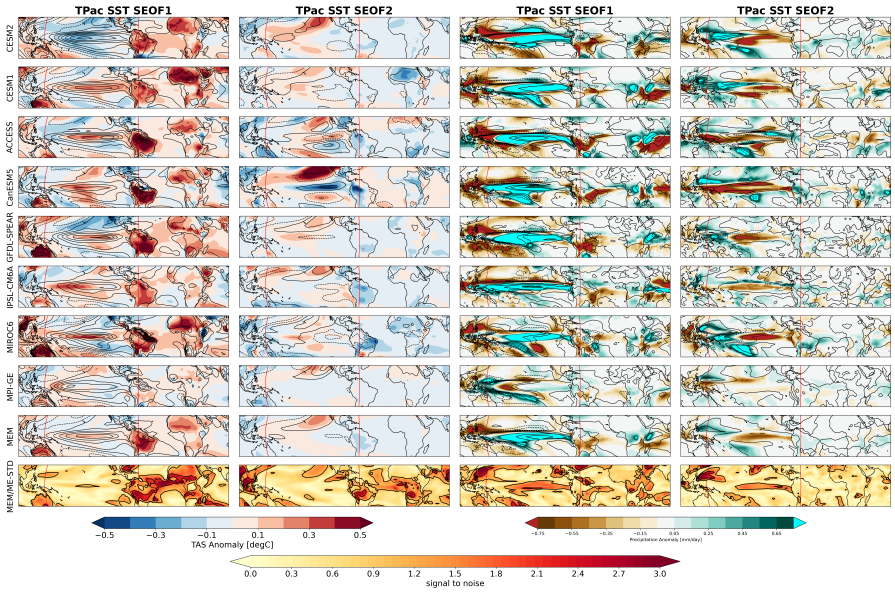


Fig. S9 Projected change in the Tropical Pacific SST SEOFs regressed onto surface air temperature and precipitation over the tropics. Each SEOF is regressed onto surface air temperature (left) and precipitation (right) in DJF. Shown is the change in this regression in 2087-2097 compared to 1924-1934. Shown for each SMILE, the multi-ensemble mean (MEM) the signal-to-noise ratio defined as the MEM divided by the standard deviation across the 8 SMILE means (ME-STD). Contours show the baseline period 1924-1934 for reference. Contours on the signal-to-noise ratio show the values 1 and 2.

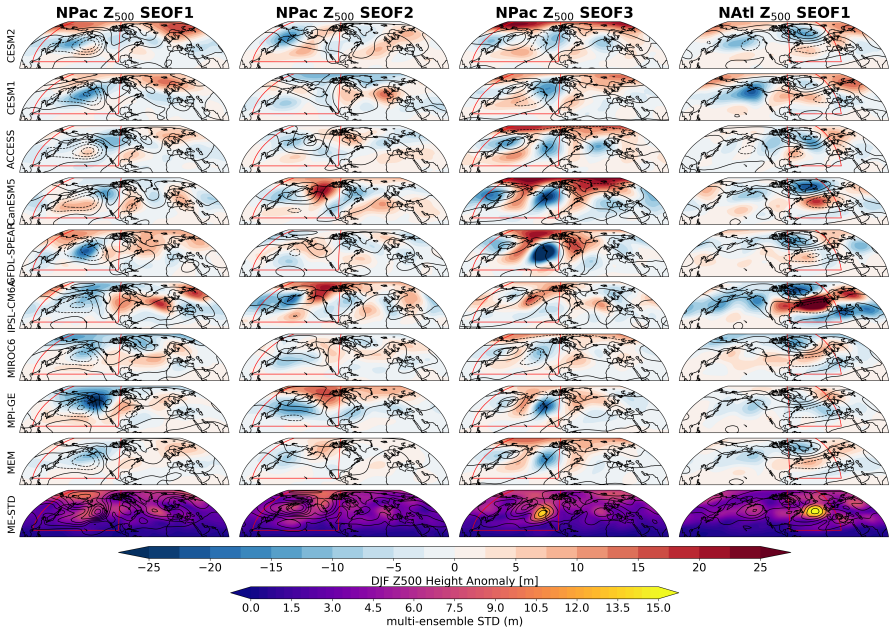


Fig. S10 Projected change in the North Pacific and North Atlantic Z500 SEOFs regressed onto Z500 after the influence of the tropical Pacific is removed. Change in each of the North Pacific SEOF1-3 and North Atlantic SEOF1 after the removal of Tropical Pacific SST SEOF1-2 as regressed onto Z500 from 2087-2097 as compared to 1924-1934. Shown for each SMILE, the multi-ensemble mean (MEM) and the standard deviation across the 8 SMILE means (ME-STD). Contours show the baseline period 1924-1934 for reference. The tropical Pacific SST SEOFs are removed using regression prior to the projected change being regressed back onto Z500.

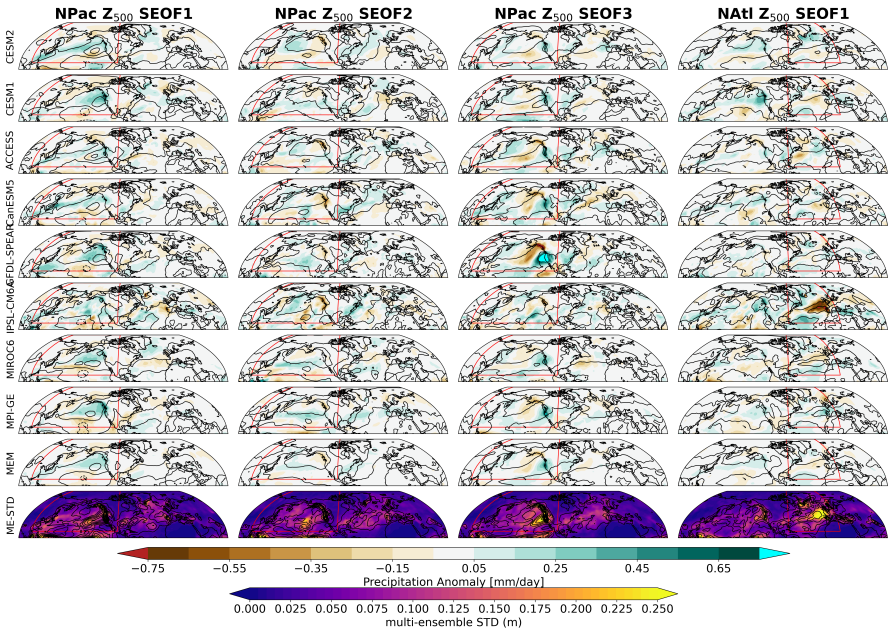


Fig. S11 Projected change in the North Pacific and North Atlantic Z500 SEOFs regressed back onto precipitation after the influence of the tropical Pacific is removed. As in Figure S10 but for precipitation.